

Effectiveness of ADC histogram analysis in the diagnosis of focal liver lesions; is a contrast agent necessary?*

Ahmet TANYERI¹, Mehmet Burak CILDAG², Omer Faruk Kutsi KOSEOGLU³

¹ Radiology Department, Yozgat City Hospital, Yozgat, Turkey

² Radiology Department, School of Medicine, Adnan Menderes University, Aydin, Turkey

³ Radiology Department, Ataturk Education and Research Hospital, Izmir Katip Celebi University, Izmir, Turkey

Corresponding Author: Ahmet TANYERI

E-mail: dr.a.tanyeri@gmail.com

Submitted: 23.11.2021

Accepted: 19.03.2022

ABSTRACT

Objective: The diagnostic success of apparent diffusion coefficient (ADC) histogram analysis in focal liver lesions, and the effects of quantitative data added to contrast-enhanced abdominal magnetic resonance imaging (MRI) on the diagnostic accuracy were investigated.

Materials and Methods: The conventional MRI findings of 524 lesions in total were retrospectively examined. Contrast enhancement kinetics and ADC values for each lesion were found through an image analysis software.

Results: Three hundred and fifty (67%) of the lesions were diagnosed as benign and 174 (33%) as malignant. Statistically significant difference was found between the benign and malignant lesion groups in terms of the minimum, maximum and mean ADC values ($p < 0.001$). When optimal thresholds for minimum, maximum and mean ADC were taken as $1.47 \times 10^{-3} \text{mm}^2/\text{s}$; $1.85 \times 10^{-3} \text{mm}^2/\text{s}$; $1.72 \times 10^{-3} \text{mm}^2/\text{s}$ respectively, sensitivity was found to be 97%; 83%; 95%, specificity was 100%; 98%; 99%, NPV was 100%; 99%; 99%, and PPV was 93%; 74%; 90%. ADC values added to MRI increased the diagnostic success for metastases (92%→96%), HCC (63%→73%), hemangioma (90%→99%) and FNH (56%→75%).

Conclusion: ADC measurement could not show reasonable success in the diagnosis of specific lesions while being successful in the differentiation of benign and malignant lesions. Minimum ADC is more successful than mean and maximum ADC. A non-contrast-enhanced MRI protocol based on the ADC measurement applicable to the selected patient group may be helpful.

Keywords: Contrast agent, Liver lesions, Diffusion weighted imaging (DWI), Apparent diffusion coefficient (ADC)

1. INTRODUCTION

The liver is the largest organ located in the abdomen having a rich vascular structure and a complex histopathological basis, in which a wide variety of lesions can be encountered. Radiological evaluations are performed using ultrasonography (US), computerized tomography (CT) and magnetic resonance imaging (MRI). MRI is superior to US and CT for the assessment of a broad spectrum of hepatic diseases due to its advantages such as high contrast resolution, ability to provide images at three planes and not requiring ionizing radiation. Being a state-of-the-art technology product and having a high diagnostic value, MRI is used today as a problem-solving, even as a first-line diagnostic

method [1, 2]. However, findings may overlap even if all data obtained for lesion characterization are combined. Intravenous gadolinium contrast agents used in MRI are known to improve diagnostic quality; however frequent use has disadvantages due to their side effects. Nephrogenic systemic fibrosis, which is a serious side effect recently identified in patients with renal failure [3-5] brought out the need for development of new MR techniques that will contribute to diagnosis without requiring the use of gadolinium. To meet this need, diffusion-weighted imaging (DWI)/apparent diffusion coefficient (ADC) without contrast agent requirement have been the subject of investigations during the recent years.

* This article was extracted from the first author's doctorate dissertation entitled "The role of diffusion weighted imaging in diagnosis and follow-up of liver masses alongside conventional MRI findings".

How to cite this article: Tanyeri A, Cildag MB, Koseoglu OFK. Effectiveness of ADC histogram analysis in the diagnosis of focal liver lesions; is a contrast agent necessary? Marmara Med J 2022; 2; 35(2):187-195. doi: 10.5472/marumj.1121815

The primary objective of this study was to determine the effectiveness of ADC histogram analysis in the diagnosis of focal liver lesions. The secondary objective was to investigate the effect of ADC values added to MRI on the diagnostic accuracy and the necessity of contrast agents.

2. MATERIALS and METHODS

Study Population

Approval was received from Adnan Menderes University, School of Medicine Ethics Committee for this retrospective study (approval number: 2017/1267). The intravenous contrast-enhanced upper abdominal MRI scans of 2212 patients aged 18 or above that had been obtained between December 2014 and December 2017 were retrospectively examined. The scans of 948 patients for which the MRI reports mentioned focal lesions in the liver were selected. The images of the selected scans were examined, and 254 that were not of optimal diagnostic quality for various reasons, could not be localized in the ADC map and/or have size of lesion smaller than 10 mm were excluded from the study. The remaining 694 scans were evaluated for eligibility using the following inclusion criteria.

Inclusion Criteria

1. Primary malignant liver tumor (hepatocellular carcinoma (HCC), intrahepatic cholangiocellular carcinoma (CCC): histopathological confirmation (needle biopsy and/or surgical specimen) is required.
2. Secondary malignant liver tumor (metastasis): histopathological confirmation and/or non-liver proven primary malignancy is required.
3. Malignant liver lesion: without any treatment.
4. Benign liver lesion: if no tissue diagnosis is available, presence of typical MR imaging findings as well as confirmation with a follow-up MRI obtained at our institution at least 6 months later and/or with other imaging modalities (US, CT) are required.
5. The number of lesions in the group is required to be greater than 10.

One hundred and two scans that did not meet the 1st and 2nd criteria above, 22 that did not meet the 3rd criterion, 30 that did not meet the 4th criterion, and 16 that did not meet the 5th criterion (6 hepatic abscesses, 5 hydatid cysts, 3 lipomas, 2 angiosarcomas) were excluded from the study. The remaining 524 scans were included in the analysis. Only 1 lesion was evaluated in each scan. If there were more than one similar lesion in the liver, the largest and/or most diagnostic (without artifacts) one were included, and if there were lesions of different structures, the malignant one was included in case of coexistence of malignant and benign lesions, and the rarer one was included in case that there were more than one benign lesion.

Magnetic Resonance Imaging

Scans were performed on a 1.5-T Achieva system (Philips Healthcare, Best, The Netherlands) in conjunction with an 8-element body coil array.

The liver image was acquired in the axial plane in all patients both before and after administration of gadoteric acid at a dose of

0.15 mL/kg. The contrast agent was automatically administered intravenously at a rate of 3 mL/s with a power injector, followed by a 25-mL saline flush.

Our institutional abdominal MRI protocol for imaging the liver included a respiration-triggered axial T1-weighted turbo field-echo in-phase sequence [repetition time/echo time (TR/TE), 10/4.6; flip angle (FA), 15°; matrix size (MS), 252x151; section thickness (ST), 7 mm] and out-of-phase sequence (TR/TE, 11/6.9; FA, 15°; MS, 252x151; ST, 7 mm), T2 weighted-turbo spin echo-high resolution (TR/TE, 484/80; FA, 90°; MS, 252x173; ST, 7 mm), axial T2 weighted-spectral attenuated inversion recovery (TR/TE, 424/80; FA, 90°; MS, 236x165; ST, 7 mm), axial balanced turbo field-echo sequence (TR/TE, 3.4/16; FA, 10°; MS, 288x226; ST, 7 mm) with a 1 – to 2-mm intersection gap, and a field of view (FOV) of 30–38 cm.

For gadoteric acid-enhanced MRI, arterial phase (20-35 s), portal phase (60 s), 3-min late phase, and 10-min delayed hepatobiliary phase images were obtained using a T1-weighted high-resolution isotropic volume examination; T1-weighted high-resolution isotropic volume excitation (THRIVE) (TR/TE, 4.2/1.98; FA, 10°; MS, 188x148) with a 2-mm section thickness and a field of view (FOV) of 30-38 cm.

Diffusion images were obtained using a free-breathing multislice spin-echo echo-planar imaging (EPI) sequence; (TR/TE, 1410/69; FA, 90°; MS, 124x99) with a 5-mm section thickness and a FOV of 30-38 cm. Three motion probing gradients with b-values of 0, 600 and 1000 s/mm² were applied in three orthogonal directions and trace images were synthesized for each b-value using the mean of three orthogonal directions. ADC maps were calculated on a pixel-by-pixel basis using a monoexponential fit, and b=0 was excluded from the calculation in order to eliminate perfusion effects.

Image Analysis

All examinations were evaluated together by two radiologists with 4 and 15 years of experience. The number of lesions for each examination was divided into three groups: single, two-five, more than five-multiple. Then the location (segment), size (the longest transvers diameter on the axial plane), margin [regular (or macrolobulated) or irregularity (microlobulated or speculated)], borders (well-defined or poorly defined) and T1, T2 signal [hypointense-hyperintense (pure or heterogeneous), isointense] of the selected lesion were recorded.

Apparent diffusion coefficient map was generated automatically by using the licensed imaging analysis software (Myrian; Intrasure, France) according to the algorithm of the equation $ADC\text{ mm}^2/\text{s} = 1/b_1 \times \ln [IS(b_0)/IS(b_1)]$. ADC measurements were performed on the map generated based on the values b=0 and b=1000. Measurements were performed by means of a manual region of interest (ROI) drawn on a single section on the axial plane to include an area as large as possible, avoiding peripheral borders. For malignant lesions, cystic/necrotic components, if any, were excluded from the measurement area (Figure 1). The minimum, maximum and mean ADC values calculated using histogram analysis were recorded. The contrast-enhancing kinetics of the lesions (type 1, persistently increasing contrast-enhancement; type 2, plateau; type 3, wash-out) were found simultaneously with the same ROI drawn.

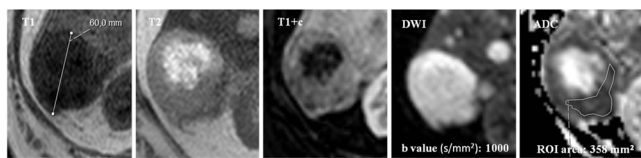


Figure 1. A 70-year-old/male/lung cancer-liver metastasis

T1 heterogeneous hypointense, T2 heterogeneous hyperintense mass in the segment 6 of the liver with lobulated contours, well-defined borders, and a necrotic degeneration area at the center, and ADC measurement method; the mean ADC $0.9 \times 10^{-3} \text{mm}^2/\text{s}$, minimum ADC: $0.5 \times 10^{-3} \text{mm}^2/\text{s}$, maximum ADC: $1.1 \times 10^{-3} \text{mm}^2/\text{s}$, contrast enhancement pattern type 1.

Statistical Analysis

The statistical analysis was conducted using the SPSS (version 21.0; SPSS Inc., Chicago, IL, USA) and MedCalc (version 18; Ostend, Belgium).

Conformance of the data to the normalized distribution was investigated using the Kolmogorov-Smirnov test. ADC values were expressed as “median (25th-75th percentile)”, and age and size were

expressed as “mean (\pm standard deviation/minimum-maximum)”. ADC values were compared between the benign and malignant groups using the Mann-Whitney U test. For these two groups, the optimal threshold, specificity, sensitivity, positive predictive value (PPV), negative predictive value (NPV) were found using the MedCalc software by applying the ROC receiver operating characteristic (ROC) analytical test. The Kruskal Wallis H test was used for the multiple group comparisons; and Post-Hoc tests were used to determine which group means were significantly different. Results with a $p < 0.05$ value were considered statistically significant.

3. RESULTS

For the 524 (242 male, 282 female) patients, the mean age was 60 ($\pm 12/21-88$) years. Among the lesions found by MRI, 350 (67%) were classified as benign and 174 (33%) as malignant tumors. Of the 350 benign lesions, 171 (49%) were diagnosed as cyst, 152 (43%) as hemangioma, 16 (5%) as focal nodular hyperplasia (FNH) and 11 (3) as hepatic adenoma (HA), while of the 174 malignant lesions, 121 (70%) were diagnosed as metastasis, 41 (24%) as hepatocellular carcinoma and 12 (6%) as cholangiocellular carcinoma.

Table I. Demographic information, MRI findings and ADC values in benign lesions

Benign Lesions		Cyst	Hemangioma	FNH	HA	Total	
Sample Size (n)		171	152	16	11	350	
Age ^a		56 ($\pm 12/25-84$)	53 ($\pm 12/21-84$)	48 ($\pm 18/43-65$)	56 ($\pm 17/25-69$)	54 ($\pm 14/21-84$)	
Male-Female		63-108	60-92	4-12	7-4	134-216	
Number of lesions	Single	105 (61%)	95 (62%)	13 (81%)	9 (82%)	222 (63%)	
	Two-Five	62 (36%)	53 (35%)	3 (19%)	2 (18%)	120 (34%)	
	>Five-Multiple	4 (3%)	4 (3%)	-	-	8 (3%)	
Selected Lesion	Dimension (mm) ^b	31 ($\pm 21/10-125$)	27 ($\pm 17/10-120$)	35 ($\pm 19/15-84$)	40 ($\pm 23/20-85$)	30 ($\pm 20/10-125$)	
	Segments	7 (35%)	7 (38%)	6 (38%)	5 (27%)	7 (37%)	
	Shape	Regular	171 (100%)	150 (99%)	13 (81%)	11 (100%)	345 (99%)
		Irregular	-	2 (1%)	3 (19%)	-	5 (1%)
	Border	Well-defined	171 (100%)	152 (100%)	16 (100%)	11 (100%)	350 (100%)
Poorly defined		-	-	-	-	-	
T1	Hypointense	171 (100%)	152 (100%)	16 (100%)	7 (64%)	346 (99%)	
	Hyperintense	-	-	-	4 (36%)	4 (1%)	
	Isointense	-	-	-	-	-	
T2	Hypointense	-	-	-	-	-	
	Hyperintense	171 (100%)	152 (100%)	10 (63%)	2 (18%)	335 (96%)	
	Isointense	-	-	6 (37%)	9 (82%)	15 (4%)	
Contrast Kinetics	No enhancement	171 (100%)	4 (3%)	-	-	175 (50%)	
	Type 1	-	123 (81%)	5 (31%)	1 (8%)	129 (37%)	
	Type 2	-	12 (8%)	11 (69%)	5 (46%)	28 (8%)	
	Type 3	-	13 (8%)	-	5 (46%)	18 (5%)	
ADC ^c ($\times 10^{-3} \text{mm}^2/\text{s}$)	Minimum	1.77 (1.70-1.94)	1.22 (1.11-1.35)	0.94 (0.81-1.05)	0.88 (0.78-1.06)	1.56 (1.17-1.77)	
	Maximum	2.35 (2.19-2.47)	1.78 (1.64-1.96)	1.67 (1.53-1.84)	1.36 (1.35-1.56)	1.96 (1.75-2.37)	
	Mean	2.05 (1.93-2.16)	1.49 (1.32-1.66)	1.26 (1.24-1.35)	1.06 (0.96-1.20)	1.77 (1.45-2.12)	

FNH: focal nodular hyperplasia, HA: hepatic adenoma

a, b: Age and dimension are presented as mean (\pm standard deviation / minimum-maximum)

c: ADC values are presented as median (25th-75th percentile)

For each subgroup within the benign and malignant lesion groups, the demographic data including age and sex distribution as well as the conventional MR findings, contrast-enhancement kinetics and ADC histogram analysis results were shown in Table I and Table II. Of the 350 (age: 54±14/21-84 years, sex: 134 male/216 female) patients with benign lesions, 222 (%63) had single lesion. The mean

size was 30 (±20/10-125) mm, and the area where such lesions were most frequently seen was the 7th segment (37%). Almost all lesions had regular margin (99%), all had well-defined borders, almost all were hypointense (99%) in T1, and hyperintense (96%) in T2. No contrast enhancement was seen in 50% of all benign lesions due to predominance of simple cysts, and the second most frequent (37%) finding was type 1 contrast enhancement (Table I).

Table II. Demographic information, MRI findings and ADC values in malignant lesions

Malignant Lesions		Metastasis	HCC	CCC	Total	
Sample Size		121	41	12	174	
Age ^a		64 (±11/34-89)	66 (±9/38-90)	65 (±10/52-78)	65 (±10/42-90)	
Male-Female		71/50	31/10	6/6	108/66	
Number of Lesions	Single	34 (28%)	19 (46%)	5 (42%)	58 (33%)	
	Two-Five	36 (30%)	8 (20%)	4 (33%)	48 (28%)	
	>Five-Multiple	51 (42%)	14 (34%)	3 (25%)	68 (39%)	
Selected Lesion	Dimension (mm) ^b	41 (±32/10-200)	70 (±45/16-195)	92 (±40/60-170)	52 (±40/10-200)	
	Segments	6 (51%)	6 (46%)	6 (50%)	6 (49%)	
	Shape	Regular	62 (51%)	14 (34%)	6 (50%)	82 (47%)
		Irregular	59 (49%)	27 (66%)	6 (50%)	92 (53%)
	Border	Well-defined	103 (82%)	34 (83%)	8 (67%)	145 (83%)
Poorly defined		18 (14%)	7 (17%)	4 (33%)	29 (17%)	
T1	Hypointense	121 (100%)	32 (77%)	12 (100%)	165 (95%)	
	Hyperintense	-	9 (23%)	-	9 (5%)	
	Isointense	-	-	-	-	
T2	Hypointense	7 (6%)	-	-	7 (%4)	
	Hyperintense	112 (92%)	32 (87%)	10 (84%)	154 (89%)	
	Isointense	2 (2%)	9 (13%)	2 (16%)	13 (7%)	
Contrast Kinetics	No enhancement	1 (1%)	-	-	1 (1%)	
	Type 1	10 (8%)	8 (19%)	-	18 (10%)	
	Type 2	26 (22%)	22 (54%)	4 (33%)	52 (30%)	
	Type 3	84 (69%)	11 (27%)	8 (67%)	103 (59%)	
ADC ^c (x10 ⁻³ mm ² /s)	Minimum	0.51 (0.45-0.60)	0.70 (0.56-0.84)	0.53 (0.52-0.55)	0.53 (0.45-0.64)	
	Maximum	1.05 (0.91-1.23)	1.20 (1-1.39)	1.22 (1.02-1.39)	1.06 (0.93-1.27)	
	Mean	0.82 (0.74-0.98)	0.91 (0.75-1.10)	0.85 (0.77-0.86)	0.84 (0.74-0.99)	

HCC: hepatocellular carcinoma, CCC: cholangiocellular carcinoma

a, b: Age and dimension are presented as mean (± standard deviation / minimum-maximum)

c: ADC values are presented as median (25th-75th percentile)

Of the 174 (age: 65±10/42-90, sex: 108 male/66 female) patients with malignant lesions, 58 (33%) had single, 48 (28%) had two to five, 68 (39%) had more than five-multiple masses. For the selected lesions, the mean size was 52 (±40/10-200) mm, and the area where such lesions were most frequently seen was the 6th segment (49%). 53% of the lesions had irregular margin, 83% had well-defined borders, almost all were hypointense (95%) in T1, and hyperintense (89%) in T2. In the dynamic contrast-enhanced series, 59% had type 3, 30% had type 2, and 10% had type 1 contrast-enhancement (Table II).

For all benign lesions, the minimum, maximum and mean ADC values were as follows; 1.56 (1.17-1.77)x10⁻³mm²/s, the, 1.96 (1.75-2.37)x10⁻³mm²/s, and was 1.77 (1.45-2.12)x10⁻³mm²/s, respectively. For all malignant lesions, the minimum, maximum and mean ADC values were as follows 0.53 (0.45-0.64)x10⁻³mm²/s, 1.06 (0.93-1.27) x10⁻³mm²/s, and 0.84 (0.74-0.99)x10⁻³mm²/s, respectively. A marked statistically significant difference in terms of ADC values was found between the benign and malignant lesion groups (p<0.001). When optimal thresholds for minimum, maximum and mean ADC were taken as 1.47x10⁻³mm²/s; 1.85x10⁻³mm²/s; 1.72x10⁻³mm²/s respectively, sensitivity was found to be 97%; 83%; 95%, specificity was 100%; 98%; 99%, NPV was 100%; 99%; 99%, and PPV was 93%; 74%; 90% (Table III). The box plots indicating the distribution of the ADC values in these two groups are shown in Figure 2.

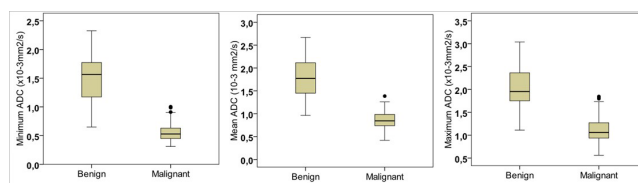


Figure 2. Box plots graphs of minimum, mean, maximum ADC values for benign and malignant lesions

When the ADC values of the lesions were compared; differences were found between cysts and other lesions and between hemangiomas and malignant lesions (p<0.001). While there was no difference for the minimum ADC values between focal nodular hyperplasia (FNH) and metastases, differences were found for the maximum and mean ADC values (p<0.001). No differences were found in the ADC values within the malignant lesions, within the benign lesions except for cysts, and additionally, no ADC difference was found between the hepatic adenomas and malignant lesions (Table IV). With the addition of quantitative ADC data, the diagnostic success of MRI increased from 92% to 96% for metastasis, from 63% to 73% for HCC, from 90% to 99% for hemangioma, and from 56% to 75% for FNH. ADC measurement had no effect on diagnostic accuracy for hepatic adenoma, simple cyst and CCC (Table V).

Table III. Effectiveness of ADC values in differentiation of benign-malignant lesion groups

ADC (x10 ⁻³ mm ² /s)	Benign (n:350)	Malignant (n:174)	P value	Cut-off value	Sensitivity (%)	Specificity (%)	NPV (%)	PPV (%)	AUC
Minimum	1.56 (1.17-1.77)	0.53 (0.45-0.64)	<0.001	1.47	97	100	100	93	0.966
Maximum	1.96 (1.75-2.37)	1.06 (0.93-1.27)	<0.001	1.85	83	98	99	74	0.948
Mean	1.77 (1.45-2.12)	0.84 (0.74-0.99)	<0.001	1.72	95	99	99	90	0.982

AUC: area under the curve, NPV: negative predictive value, PPV: positive predictive value

Table IV. Comparison of ADC values among focal liver lesions

Lesion Groups	Benign				Malignant			P value
	Cyst	Hemangioma	FNH	HA	Metastasis	HCC	CCC	
Sample Size	171 (33%)	149 (28%)	16 (3%)	11 (2%)	121 (23%)	41 (8%)	12 (3%)	
ADC Minimum	1.77 (1.70-1.94)	1.22 (1.11-1.35)	0.94 (0.81-1.05)	0.88 (0.78-1.06)	0.51 (0.45-0.6)	0.70 (0.56-0.84)	0.53 (0.52-0.55)	<0.001 ^a
ADC Maximum	2.35 (2.19-2.47)	1.78 (1.64-1.96)	1.67 (1.53-1.84)	1.36 (1.35-1.56)	1.05 (0.91-1.23)	1.20 (1-1.39)	1.22 (1.02-1.39)	<0.001 ^b
ADC Mean	2.05 (1.93-2.16)	1.49 (1.32-1.66)	1.26 (1.24-1.35)	1.06 (0.96-1.20)	0.82 (0.74-0.98)	0.91 (0.75-1.10)	0.85 (0.77-0.86)	<0.001 ^c

FNH: focal nodular hyperplasia, HA: hepatic adenoma, HCC: hepatocellular carcinoma, CCC: cholangiocellular carcinoma

ADC values are presented as median (25-75th percentile)

a: For minimal ADC, there was a significant difference between cyst-other lesions and hemangioma-malignant tumors

b, c: For maximum and mean ADC, there was a significant difference between cyst-other lesions, hemangioma-malignant tumors and FNH-metastasis

Table V. Effect of ADC values measured in focal liver lesions on the diagnostic success of MRI

Final Diagnosis	n	MRI		Ratio	Between Groups ADC Difference	Diagnostic Success Rate Before ADC–After ADC
		Diagnosis	n			
Metastasis	121	Metastasis	111	92%		92% → 96%
		HCC	4	3%	n.s.	
		Hemangioma	5	4%	p<0.001	
		CCC	1	1%	n.s.	
HCC	41	HCC	26	63%		63% → 73%
		Metastasis	9	22%	n.s.	
		Hemangioma	4	10%	p<0.001	
		KSK	2	5%	n.s.	
CCC	12	CCC	3	25%		25% – 25%
		Metastasis	8	67%	n.s.	
		HCC	1	8%	n.s.	
Cyst	171	Cyst	171	100%		100% – 100%
Hemangioma	152	Hemangioma	137	90%		90% → 99%
		Metastasis	14	9%	p<0.001	
		FNH	1	1%	n.s.	
FNH	16	FNH	9	56%		56% → 75%
		Hemangioma	4	25%	n.s.	
		Metastasis	3	19%	p<0.001*	
Hepatic Adenoma	11	Hepatic adenoma	7	64%		64% – 64%
		Metastasis	3	27%	n.s.	
		Hemangioma	1	3%	n.s.	

n.s.: no significant difference

FNH: focal nodular hyperplasia, HCC; hepatocellular carcinoma, CCC: cholangiocellular carcinoma

* Statistical difference was found for mean and maximum ADC

4. DISCUSSION

Diffusion-weighted imaging exploits the regional differences in the motion of water molecules within the extracellular/extravascular compartment of tissues. In highly cellular tissues (e.g., lymphoma, carcinoma and abscess), the compact nature of the extracellular space causes increased impediment to motion of water molecules and the resultant water diffusion in such tissues is said to be “restricted”. On the contrary, in tissues that are necrotic or fluid filled (e.g., cysts), there is unrestricted motion of water molecules and water diffusion in such tissues, which is said to be “free”. Therefore, the diffusion properties in different tissues provide information on tissue cellularity and the integrity of cellular membranes [6, 7]. Because of the relatively short T2 relaxation time of the normal liver parenchyma, the b values used for clinical diffusion imaging are typically no higher than 1000 sec/mm² [6]. To generate b values larger than this would generally require the use of longer diffusion-gradient pulses with longer echo times. In this case, the image distortion associated with T2 decay and the echoplanar imaging technique itself is prone to increase further with increasing b values. Moreover, there is a tendency to loss of image signal [8]. ADC is the measurable parameter of the tissue water diffusion properties obtained from DWI.

There are studies in the literature on benign-malignant differentiation and subgroup characterization in liver lesions using ADC [Table VI, 9-13]. In these studies, different success rates were reported using various ADC thresholds showing variability most

probably due to factors such as differences in the parameters used to obtain ADC maps, or the measurement technique etc. However, the common view is that ADC values are higher in benign and lower in malignant liver lesions. In our study, the mean ADC threshold was slightly higher than in the mentioned studies; however it appears to be more successful in benign-malignant differentiation.

In our study, the minimum and maximum ADC values were found by histogram analysis in addition to frequently used mean ADC. Minimum ADC represents the most proliferative area with the highest cellularity in tumors of heterogeneous structure [14]. On the other hand, maximum ADC which is the opposite of this, indicates the area with the lowest cellularity with the highest extracellular fluid concentration. There are studies demonstrating that minimum ADC is an effective parameter for benign-malignant differentiation and tumor grading in breast and brain tumors [14-17]. While we could not find a similar study for liver masses in the literature, minimum ADC was markedly more successful compared to maximum ADC while being slightly more successful compared to mean ADC. Although, the cystic/necrotic component is avoided during measurement, sometimes this may not be possible. This component becomes harder to notice with the decreased size of lesion. Removing focal necrotic areas distributed within solid areas during measurement may be technically difficult, even impossible. This aspect of ADC measurement for which standardization is being attempted may vary from person to person. The fact that minimum ADC represents the

area with the highest cellularity in the mixed structure appears to be helpful both for differentiation and measurement standardization.

There are studies suggesting that using ADC alone for characterization of liver lesions should be avoided and this method should be used in combination with conventional MR sequences [18-20]. On the other hand, some studies reported that ADC values overlap between solid benign and malignant lesions [21, 22]. Based on the results of our study, we concluded that ADC measurement alone is not enough for specific lesion characterization beyond benign-malignant differentiation. Only simple cysts could be differentiated from other benign lesions with significantly high ADC values. However, for the diagnosis of a benign lesion such as a simple cyst that can be easily identified using conventional sequences, ADC measurement will not be practical in routine practice. But ADC measurement can provide a major contribution to the diagnostic success in case of suspect in the diagnosis of hemangioma that is also benign, commonly seen, and may be confused with malignant lesions such as metastases due to atypical staining and signal characteristics. It should be noted that solid benign lesions such as hemangioma, FNH and hepatic adenoma can show restricted diffusion compared to normal liver parenchyma. This restriction is substantially lower than in malignant lesions, but the difference may not be noticeable to naked eye in DWI/ADC evaluation. In their recent study, Zarghampour et al., reported that ADC is successful in HA-HCC and HA-FNH differentiation while being unsuccessful in FNH-HCC differentiation [23]. Similar to the mentioned study, our study found that ADC is unsuccessful in FNH-HCC differentiation. On the contrary, ADC could not be successful in the differentiation of hepatic adenoma from other benign and malignant tumors.

Studies were conducted to investigate the diagnostic utility of DWI compared to contrast-enhanced series especially in oncology patients with impaired renal function [24-28]. Hardie et al., reported that contrast-enhanced T1 sequence and DWI show similar success in the differentiation of metastatic and benign liver lesions, and DWI can be used as an alternative to contrast-enhanced MRI [29]. On the contrary, in a similar study Donati et al., reported that DWI alone has a diagnostic accuracy lower than contrast-enhanced MRI, it cannot be used alone and may be helpful only to ensure diagnostic reliability [30]. DWI-ADC is evaluated only qualitatively in our institution. With the added quantitative ADC data, the diagnostic accuracy of MRI increased for metastasis, HCC, hemangioma and FNH. It was found that the mostly confused lesion in benign-malignant differentiation is hemangioma. It was seen that 5 (4%) of 121 metastatic lesions and 4 (10%) of 41 HCCs had been reported as hemangiomas while 14 (9%) of 152 hemangiomas had been reported as metastases. When the examinations were re-evaluated, we observed that the major cause for this is the contrast enhancement pattern. The typical contrast enhancement pattern expected in hemangioma is not always seen and is non-specific (Fig. 3). Based on our results, we can say that the most effective use of ADC is in the differentiation of hemangioma and malignant tumor. The areas with the lowest diagnostic success of MRI were CCC (25%) followed by FNH

(56%), HCC (63%) and HA (64%). The contrast enhancement pattern for the diagnosis of FNH and HA was non-specific, and the expected morphological signs were insufficient. Use of a hepatocyte-specific contrast agent appears to be necessary particularly in the diagnosis and differentiation of these two lesions [31]. The diagnostic success was low for CCC and HCC because of confusion with metastases. After administration of contrast agent, CCC shows centripetal contrast enhancement following continuous thick annular peripheral opacification during the early arterial phase. During the late portal venous phase, progressive heterogeneous contrast enhancement associated with late contrast enhancement of internal fibrous tissue. However, this contrast enhancement pattern is non-specific [32]. Only 33% of the CCCs in our study showed this opacification pattern. The diagnostic effect of contrast-enhanced series cannot be ignored but may sometimes be confusing. Moreover, the toxic effect resulting from exposure to contrast agent causes benefit-harm dilemma. We think that an MRI protocol based on non-contrast/-enhanced and quantitative ADC measurement applicable to the selected patient group may be sufficient for benign-malignant differentiation which is the most important point.

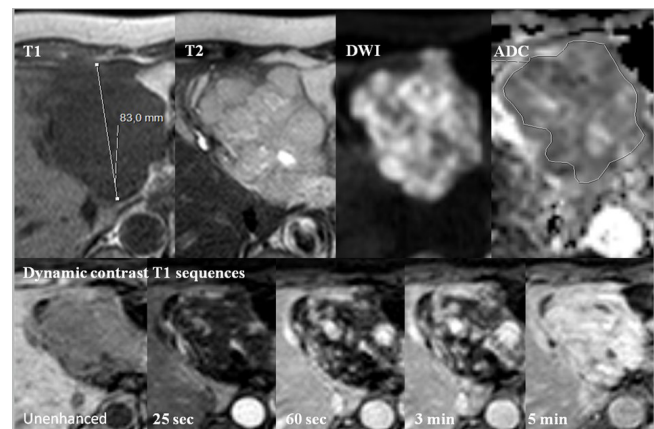


Figure 3. A 68-year-old/female/well-differentiated HCC confused with hemangioma

T1 hypointense, T2 heterogeneous hyperintense mass in the segment 3 of the liver with lobulated contours and well-defined borders, which becomes opacified with centripetal nodular enhancement and contrast-enhanced during the late phase; mean ADC $1.1 \times 10^{-3} \text{mm}^2/\text{s}$, minimum ADC: $0.9 \times 10^{-3} \text{mm}^2/\text{s}$, maximum ADC: $1.4 \times 10^{-3} \text{mm}^2/\text{s}$, contrast enhancement pattern type 2. Even if the lesion morphology and staining pattern mimic hemangioma, malignant tumor is considered with the contribution of ADC measurement.

There are some limitations in this study. Some lesion groups were of limited number with limited lesion types. The ADC measurement method and the b value used may be questionable. There is no consensus in the literature on this issue. The ADC measurements were performed by two radiologists together; the reproducibility of them may be questionable.

In conclusion; although, no reasonable success was found for determining the lesion subtypes of malignant cases, ADC

measurement in focal liver lesions was found to be successful in the differentiation of benign and malignant lesions. The diagnostic success of minimum ADC was found to be higher and appears to be more suitable for measurement standardization. In the future, standardized minimum ADC data may find a place for itself as a useful biomarker in the routine practice.

Compliance with Ethical Standards

Ethical approval: Approval was received from Adnan Menderes University, School of Medicine Ethics Committee for this retrospective study (approval number: 2017/1267). The procedures used in this study adhere to the tenets of the Declaration of Helsinki.

Funding: The authors did not receive support from any organization for the submitted work.

Conflicts of interest/competing interests: The authors have no relevant financial or non-financial interests to disclose.

Author contribution: AT: Conceived and designed the analysis, wrote the paper, MBC: Contributed data and critical analysis, OFKK:Planned the study and analyzed the data. ALL authors contributed to the final version of the manuscript.

REFERENCES

- [1] Fowler KJ, Brown JJ, Narra VR. Magnetic resonance imaging of focal liver lesions: approach to imaging diagnosis. *Hepatology* 2011; 54:2227-37. doi: 10.1002/hep.24679
- [2] Coenegrachts K. Magnetic resonance imaging of the liver: New imaging strategies for evaluating focal liver lesions. *World J Radiol* 2009; 1:72-85. doi: 10.4329/wjr.v1.i1.72
- [3] Gandhi SN, Brown MA, Wong JG, Aguirre DA, Sirlin CB. MR contrast agents for liver imaging: What, When, How. *Radiographics* 2006; 26:1621-36. doi: 10.1148/rg.266065014
- [4] Juluru K, Vogel-Claussen J, Macura KJ, Kamel IR, Steever A, Bluemke DA. MR imaging in patients at risk for developing nephrogenic systemic fibrosis: protocols, practices, and imaging techniques to maximize patient safety. *Radiographics* 2009; 29:9-22. doi:10.1148/rg.291085072
- [5] Semelka RC, Ramalho M, AlObaidy M, Ramalho J. Gadolinium in Humans: A Family of Disorders. *Am J Roentgenol* 2016; 207: 229-233. doi: 10.2214/AJR.15.15842
- [6] Taouli B, Koh DM. Diffusion-weighted MR Imaging of the Liver. *Radiology* 2010; 254:47-66. doi: 10.1148/radiol.09090021
- [7] Bammer R. Basic principles of diffusion weighted imaging. *Eur J Radiol* 2003; 45:169-84. doi: 10.1016/s0720-048x(02)00303-0
- [8] Kim T, Murakami T, Takahashi S, Hori M, Tsuda K, Nakamura H. Diffusion-weighted single-shot echoplanar mr imaging for liver disease. *Am J Roentgenol* 1999; 173:393-8. doi: 10.2214/ajr.173.2.10430143
- [9] Parsai A, Zerizer I, Roche O, Gkoutzios P, Miquel ME. Assessment of diffusion-weighted imaging for characterizing focal liver lesions. *Clin Imaging* 2015; 39:278-84. doi: 10.1016/j.clinimag.2014.09.016
- [10] Parikh T, Drew SJ, Lee VS, et al. Focal liver lesion detection and characterization with diffusion-weighted MR imaging: comparison with standard breath-hold T2-weighted imaging. *Radiology* 2008; 246:812-22. doi: 10.1148/radiol.246.307.0432
- [11] Bruegel M, Holzapfel K, Gaa J, et al. Characterization of focal liver lesions by ADC measurements using a respiratory triggered diffusion-weighted single-shot echo-planar MR imaging technique. *Eur Radiol* 2008; 18:477-85. doi: 10.1007/s00330.007.0785-9
- [12] Miller FH, Hammond N, Siddiqi AJ, et al. Utility of diffusion-weighted MRI in distinguishing benign and malignant hepatic lesions. *J Magn Reson Imaging* 2010; 32:138-47. doi: 10.1002/jmri.22235
- [13] Holzapfel K, Bruegel M, Eiber M, et al. Characterization of small (≤ 10 mm) focal liver lesions: value of respiratory-triggered echo-planar diffusion-weighted MR imaging. *Eur J Radiol* 2010; 76: 89-95. doi: 10.1016/j.ejrad.2009.05.014
- [14] Hirano M, Satake H, Ishigaki S, Ikeda M, Kawai H, Naganawa S. Diffusion-weighted imaging of breast masses: comparison of diagnostic performance using various apparent diffusion coefficient parameters. *Am J Roentgenol* 2012; 198:717-22. doi: 10.2214/AJR.11.7093
- [15] Kitis O, Altay H, Calli C, Yuntun N, Akalin T, Yurtseven T. Minimum apparent diffusion coefficients in the evaluation of brain tumors. *Eur J Radiol* 2005; 55:393-400. doi: 10.1016/j.ejrad.2005.02.004
- [16] Lee EJ, Lee SK, Agid R, Bae JM, Keller A, Terbrugge K. Preoperative grading of presumptive lowgrade astrocytomas on MR imaging: diagnostic value of minimum apparent diffusion coefficient. *Am J Neuroradiol* 2008; 29:1872-7. doi: 10.3174/ajnr.A1254
- [17] Murakami R, Hirai T, Sugahara T, et al. Grading astrocytic tumors by using apparent diffusion coefficient parameters: superiority of a oneversus two-parameter pilot method. *Radiology* 2009; 251:838-45. doi: 10.1148/radiol.251.308.0899
- [18] Park HJ, Kim SH, Jang KM, Lee SJ, Park MJ, Choi D. Differentiating hepatic abscess from malignant mimickers: value of diffusion-weighted imaging with an emphasis on the periphery of the lesion. *J Magn Reson Imaging* 2013; 38:1333-41. doi: 10.1002/jmri.24112
- [19] Wei C, Tan J, Xu L, et al. Differential diagnosis between hepatic metastases and benign focal lesions using DWI with parallel acquisition technique: a metaanalysis. *Tumour Biol* 2015; 36:983-90. doi: 10.1007/s13277.014.2663-9
- [20] Lee NK, Kim S, Kim DU, et al. Diffusion-weighted magnetic resonance imaging for non-neoplastic conditions in the hepatobiliary and pancreatic regions: pearls and potential pitfalls in imaging interpretation. *Abdom Imaging* 2015; 40:643-62. doi: 10.1007/s00261.014.0235-5
- [21] Parsai A, Zerizer I, Roche O, Gkoutzios P, Miquel ME. Assessment of diffusion-weighted imaging for characterizing focal liver lesions. *Clin Imaging* 2015; 39:278-84. doi: 10.1016/j.clinimag.2014.09.016
- [22] Taouli B, Vilgrain V, Dumont E, Daire JL, Fan B, Menu Y. Evaluation of liver diffusion isotropy and characterization

- of focal hepatic lesions with two single-shot echo-planar MR imaging sequences: prospective study in 66 patients. *Radiology* 2003; 226: 71-8. doi: 10.1148/radiol.226.101.1904
- [23] Zarghampour M, Fouladi DF, Pandey A, et al. Utility of volumetric contrast-enhanced and diffusion-weighted MRI in differentiating between common primary hypervascular liver tumors. *J Magn Reson Imaging* 2018; 48:1080-90. doi: 10.1002/jmri.26032.
- [24] Löwenthal D1, Zeile M, Lim WY, et al. Detection and characterisation of focal liver lesions in colorectal carcinoma patients: comparison of diffusion-weighted and Gd-EOB-DTPA enhanced MR imaging. *European Radiology* 2011; 21:832-40. doi: 10.1007/s00330.010.1977-2
- [25] Shimada K, Isoda H, Hirokawa Y, Arizono S, Shibata T, Togashi K. Comparison of gadolinium-EOB-DTPA-enhanced and diffusion-weighted liver MRI for detection of small hepatic metastases. *European Radiology* 2010; 20:2690-8. doi: 10.1007/s00330.010.1842-3
- [26] Colagrande S, Castellani A, Nardi C, Lorini C, Calistri L, Filippone A. The role of diffusion-weighted imaging in the detection of hepatic metastases from colorectal cancer: A comparison with unenhanced and Gd-EOB-DTPA enhanced MRI. *Eur J Radiol* 2016; 85:1027-34. doi: 10.1016/j.ejrad.2016.02.011
- [27] Kim YK, Lee YH, Kwak HS, Kim CS, Han YM. Detection of liver metastases: gadoxetic acid-enhanced three-dimensional MR imaging versus ferucarbotran-enhanced MR imaging. *Eur J Radiol* 2010; 73:131-6. doi: 10.1016/j.ejrad.2008.09.027
- [28] Zech CJ, Grazioli L, Jonas E. Health-economic evaluation of three imaging strategies in patients with suspected colorectal liver metastases: Gd-EOB-DTPA-enhanced MRI vs. extracellular contrast media-enhanced MRI and 3-phase MDCT in Germany, Italy and Sweden. *Eur Radiol* 2009; 19:753-63. doi: 10.1007/s00330.009.1432-4
- [29] Hardie AD, Naik M, Hecht EM, et al. Diagnosis of liver metastases: value of diffusion-weighted MRI compared with gadolinium-enhanced MRI. *Eur Radiol* 2010; 20:1431-41. doi: 10.1007/s00330.009.1695-9
- [30] Donati OF, Fischer MA, Chuck N, Hunziker R, Weishaupt D, Reiner CS. Accuracy and confidence of Gd-EOB-DTPA enhanced MRI and diffusion-weighted imaging alone and in combination for the diagnosis of liver metastases. *Eur Radiol* 2013; 82:822-8. doi: 10.1016/j.ejrad.2012.12.005
- [31] Roux M, Pigneur F, Calderaro J, et al. Differentiation of focal nodular hyperplasia from hepatocellular adenoma: Role of the quantitative analysis of gadobenate dimeglumine-enhanced hepatobiliary phase MRI. *J Magn Reson Imaging* 2015; 42:1249-58. doi: 10.1002/jmri.24897
- [32] Fowler KJ, Brown JJ, Narra VR. Magnetic resonance imaging of focal liver lesions: approach to imaging diagnosis. *Hepatology* 2011; 54:2227-37. doi: 10.1002/hep.24679